Synthesis, Crystal Structure, EPR, and DFT Studies of an Unusually Distorted Vanadium(II) Complex

Journal:	*Dalton Transactions*
Manuscript ID	DT-COM-07-2022-002392
Article Type:	Communication
Date Submitted by the Author:	22-Jul-2022
Complete List of Authors:	Bonitatibus, Peter; Rensselaer Polytechnic Institute, Chemistry Alvarez, Santiago; Universitat de Barcelona, Department de Quimica Inorganica Armstrong, William; Boston College Baldansuren, Amgalanbaatar; Rensselaer Polytechnic Institute, Chemistry and Chemical Biology Gaspard, Mallory; Cornell University, Center for Applied Mathematics Lakshmi, K.; Rensselaer Polytechnic Institute, Chemistry and Chemical Biology Ziegler, Micah; Massachusetts Institute of Technology, Institute for Data, Systems, and Society; Charles, Philip; Rensselaer Polytechnic Institute, Chemistry and Chemical Biology

Synthesis, Crystal Structure, EPR, and DFT Studies of an Unusually Distorted Vanadium(II) Complex

Philip Charles,[a,b] Mallory E. Gaspard,[a,b] Santiago Alvarez,[c] Micah S. Ziegler,[d] Amgalanbaatar Baldansuren,[a,b] William H. Armstrong,[e] K. V. Lakshmi,[a,b,*] and Peter J. Bonitatibus Jr.[a,*]

We report a synthesis and structure of the most highly distorted four-coordinate d³ ion known to date that also serves as the second known example of a bis(biphenolato) transition metal complex. We demonstrate the application of density functional theory to calculate the magnetic parameters derived from the experimental and simulated EPR spectra.

Interest in the development of divalent vanadium coordination chemistry featured in a biphenolate ligand donor environment stems from the discovery that systems incorporating V^{II} complexes with related anionic oxygen donor-atom ligands display interesting reactivity, such as nitrogen fixation processes[1-8] and the catalytic conversion of dinitrogen and hydrazine to ammonia.[9,10]

An investigation by Becker and Posin demonstrated that aromatic dihydroxy derivatives with V^{II} generated *in situ* were capable of dinitrogen fixation.[3] Conditions reported for the conversion required methanolic solutions of V^{II} with 1,2-, 2,3-, or 1,8-dihydroxynaphthalenes (along with 2,3-dihydroxy-quinoxaline) in the presence of excess base, such as sodium or lithium methoxide at room temperature and ambient pressure. However, the original study lacked characterization of the reactive or resultant metal-containing species, presumably due in part to the degradation of the N_2-fixing system *via* proton reduction in a protic solvent.

Otherwise motivated on the above grounds to study the coordination chemistry of V^{II} biphenolates, there has been recent interest in the preparation of coordinatively unsaturated V^{II} species that are expected to be reactive towards a variety of reducible substrates given the precedence and significance of dinitrogen chemistry. In recent years, sterically encumbered amido ligands have been used to prepare unprecedented examples of stable two and three-coordinate V^{II} compounds.[11,12]

In this report, we demonstrate the approach of using an aprotic environment for the preparation of V^{II} biphenolates that eliminates possible decomposition of initial reactive species due to proton reduction when otherwise formed in a protic solvent. Additionally, our approach of incorporating bulky biphenolate ligands permitted the preparation of a four-coordinate V^{II} compound with an unusual geometry which allowed for detailed structural and spectroscopic characterization and preliminary reactivity studies. Results of a DFT study demonstrated *ab initio* calculation of the magnetic parameters
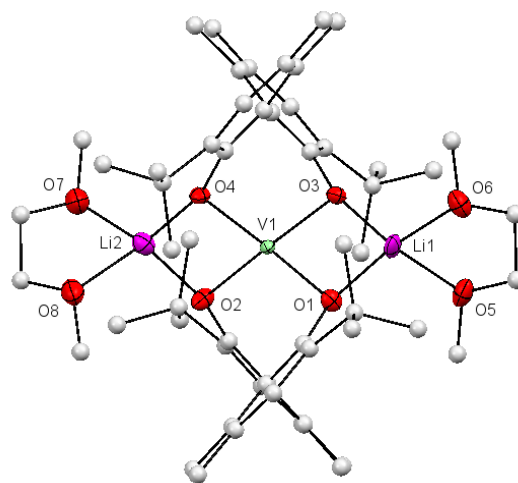

Figure 1. The X-ray crystal structure of compound **1** with thermal ellipsoids at 50% probability of all non-carbon atoms for clarity (hydrogen atoms omitted). Selected interatomic bond lengths [Å] and angles [deg]: V1-O4 1.991(5), V1-O3 2.001(5), V1-O1 2.013(5), V1-O2 2.011(6), V1··Li2 2.78(2), V1··Li1 2.81(1), O3-Li1 1.86(1), O2-Li2 1.91(2), O1-Li1 1.92(2), O4-Li2 1.83(2), O5-Li1 2.04(1), O7-Li2 1.97(2), O1-V1-O2 108.6(2), O3-V1-O4 109.8(2), O1-V1-O3 84.5(2), O2-V1-O4 84.3(2), O1-V1-O4 139.51(8), O2-V1-O3 140.98(8), Li2-V1-Li1 177.9(6), O3-Li1-O1 91.3(6), O6-Li1-O5 81.1(5), O4-Li2-O2 92.0(7), O7-Li2-O8 81.2(6).

a. *Department of Chemistry and Chemical Biology, Rensselaer Polytechnic Institute, Troy, NY 12180 USA*

b. *Baruch '60 Center for Biochemical Solar Energy Research, Rensselaer Polytechnic Institute, Troy, NY 12180 USA*

c. *Department de Química Inorgànica i Orgànica i Institut de Química Teòrica i Computacional, Universitat de Barcelona, Martí i Franquès 1-11, 08028 Barcelona Spain*

d. *Institute for Data, Systems and Society, Massachusetts Institute of Technology, Cambridge, MA 02139 USA*

e. *Department of Chemistry, Boston College, Chestnut Hill, MA 02467 USA*

obtained from the experimental and simulated EPR spectra of the V^{II} compound.

The featured compound was prepared by reacting 0.23 g (0.63 mmol) of dilithiated 3,3'-di-*tert*-butyl-5,5',6,6'-tetramethyl-1,1'-biphenyl-2,2'-diol racemic ligand (Li$_2$TBDMPD)† with 0.2 g (0.31 mmol) of an infrequently used and not often referenced V^{II} starting material, [V(THF)$_4$(CF$_3$SO$_3$)$_2$],‡ in rigorously dried THF solution. The reaction mixture changed colour from sky blue to a light brown homogeneous solution, was stirred overnight, pumped to dryness, extracted with a minimum amount of Et$_2$O to remove Li(CF$_3$SO$_3$), and subsequently filtered. Removal of solvent resulted in [V(TBDMPD)$_2$\{Li(THF)\}$_2$]·2Et$_2$O solid in 78% yield as characterized by elemental analysis and spectroscopic measurements.† Cooling the Et$_2$O filtrate described above for 12 h at 0° C with a small added amount of dimethoxyethane (DME) formed dichroic green-brown blocks of **1** as [V(TBDMPD)$_2$\{Li(DME)\}$_2$]·2Et$_2$O that were suitable for X-ray crystallography.

The crystal structure of **1** is presented in **Figure 1** with a list of selected bond distances and bond angles.† The average V^{II}-O bond distance of 2.004 Å in **1** is nearly identical (0.02 Å shorter) to the corresponding distance in the four-coordinate tetrakis(2,6-diisopropylphenolate) V^{II} analogue, [V(DIPP)$_4$\{Li(THF)\}$_2$].[13] However, in stark contrast to the nearly square planar configuration of [V(DIPP)$_4$\{Li(THF)\}$_2$], compound **1** is significantly distorted away from a square planar geometry. As a consequence of steric crowding imposed by 6,6'-methyl substituents in the TBDMPD^{2-} ligand, the aromatic rings are observed to be almost perpendicular (average 84.3°) and the anionic oxygen donors around V^{II} are arranged in a geometry that is approximately halfway between a square planar and tetrahedral configuration. Moreover, the binding of the \{Li(DME)\}$^+$ moieties stabilize compound **1** given the short average Li-O$_{phenolate}$ bond distance of 1.88 Å and contribute to the distortion of V^{II} coordination environment through the observed acute O-V-O bond angles, e.g., VO$_2$Li (ring oxygens), with values of 84.3° and 84.5°, compared to biphenolate bite angles of 108.6° and 109.8°.

In order to completely define the distortion in compound **1**, we use V1-O1 as a reference vector and select a second oxygen atom to automatically define two intersecting planes. Selection of O2 defines two intersecting planes O1-V1-O2 and O3-V1-O4 that form an angle of 49.3° (biphenolate 'bite planes'), while the selection of O3 defines planes O1-V1-O3 and O2-V1-O4 with an angle of 60.8° (VO$_2$Li planes), and finally selection of O4 defines the planes O1-V1-O4 and O2-V1-O3 that form an angle of 76.1°. Although a few mononuclear four-coordinate V^{II} species have been structurally characterized previously (*vide infra*), compound **1** is the only distorted tetrahedral case and, to our knowledge, only the second structurally characterized bis(biphenolato) transition metal complex to be reported in literature. The other transition metal species is a Zn^{II} compound that features two 3,3',5,5'-tetra-*tert*-butyl substituted biphenolate ligands.[14] In the structurally related Zn^{II} analogue, the corresponding plane angles are more obtuse; the angle made by biphenolate bite planes is 56.7°, ZnO$_2$Li planes is 66.6°, and the angle between the remaining intersecting planes is 78.8°.

Stereochemical analysis of compound **1** revealed that it is the most highly distorted tetracoordinate d^3 ion that is known to date. **Figure 2** displays a shape map[15] for structures of tetra-coordinated d^3 metal complexes in the Cambridge Structural Database (CSD).[16],† The continuous curved-line connecting the axes represents the minimum distortion path between an ideal square planar (SP-4) and tetrahedral (T-4) geometry, S(SP-4) = 0.00 and S(T-4) = 0.00, respectively. Compound **1** places very close to the minimum

distortion path with a deviation of 7%, practically midway between the two ideal geometries (i.e., a tetrahedron flattened by 47% towards square planar), which renders it the most distorted of the d^3 ions and of all tetracoordinate vanadium compounds in any oxidation state.† The only other proximal V^{II} structure in the compiled shape map in **Figure 2** corresponds to a bis(diamido) complex by Cummins and co-workers that deviates by 16% from the path.[17] All other V^{II} structures are closer to either a tetrahedral or a square planar geometry. Nearly square planar geometries are favored by ^iPr or ^tBu substituents in the proximity of the donor atoms, namely [V(DIPP)$_4$\{Li(THF)\}$_2$] which is 77% planarized[13] and a bis(phenolate)bis(pyridine) V^{II} derivative that is practically square planar,[18] or by a tridentate pincer ligand.[9] A theoretical study predicted such intermediate geometries for S = 3/2 d^3 systems and calculations on a model tetramethyl V^{II} complex presented 41% planarization, with barely a 2% deviation from the minimal distortion path.[19]

Continuous-wave (*cw*) X-band electron paramagnetic resonance (EPR) spectroscopy was used to explore the electronic structure of compound **1**. The central V^{II} ion of compound **1** has a d^3 electronic state and its EPR spectra serve as a sensitive probe of the environment surrounding the metal center. The *cw* EPR spectrum of [V(TBDMPD)$_2$\{Li(THF)\}$_2$] in THF at 4 K (black trace) and the corresponding numerical simulation (red trace) are shown in **Figure 3**. A frozen solution of compound **1** displays an EPR spectrum with two features centered at a magnetic field, B, of 175 mT and 335 mT. The spectrum is characteristic of a Kramers half-integer electron spin S = 3/2 species. Moreover, the low- and high-field spectral features in **Figure 3** display an 8-line splitting pattern that arises from the
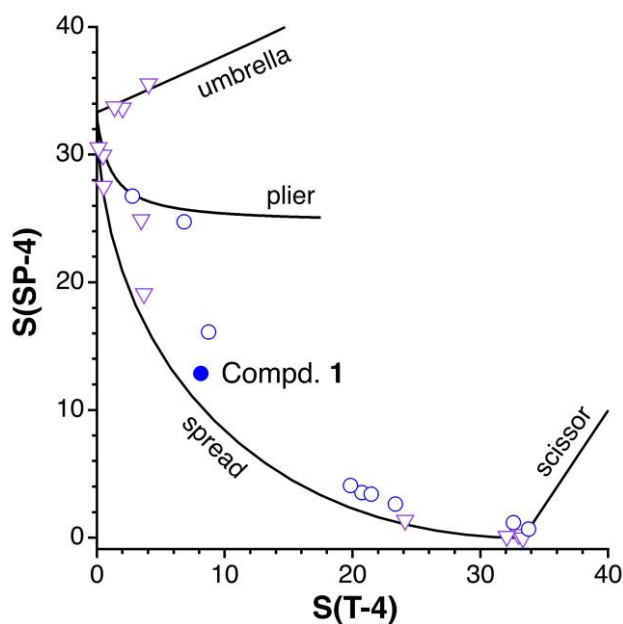

Figure 2. Distribution of tetracoordinate d^3 structures by their continuous shape measures (CSMs)[15] derived from the X-ray data in the Cambridge Structural Database (CSD).[16] The lines corresponding to different distortions of ideal square planar or tetrahedral geometries are labelled, e.g. plier, umbrella. Compound **1** is practically midway between ideal square planar and tetrahedral geometries and very close to the spread minimal distortion path exhibiting only a 7% deviation. Circles correspond to vanadium(II), triangles to other d^3 ions.
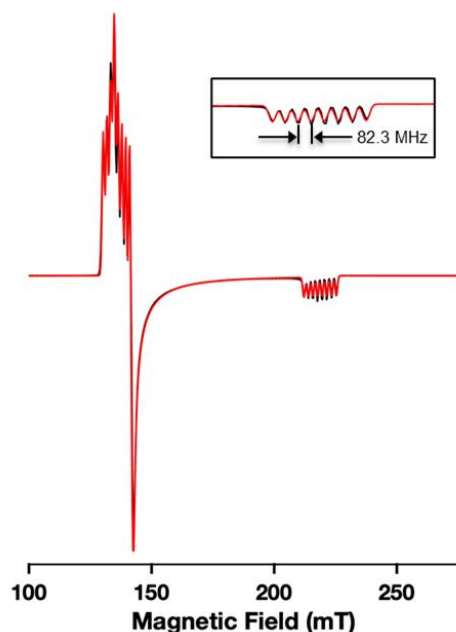
Figure 3. The X-band experimental (black) and simulated (red) continuous-wave EPR spectrum of compound **1**. Shown as an inset is the high-field '8-line pattern' of hyperfine splittings from the magnetic coupling of the electron spin, S, of 3/2 and nuclear spin, I, of 7/2 of the central $^{51}V^{II}$ ion. The experimental spectrum was acquired at a temperature of 4 K at an operating microwave frequency of 9.660 GHz with modulation frequency and amplitude of 100 kHz and 0.4 mT, respectively. The $^{51}V^{II}$ spectral simulations yielded ZFS parameters, D and E (2.66 cm^{-1} and 0.058 cm^{-1}), and a hyperfine **A**-tensor [-108, -55, -84] MHz.

electron-nuclear hyperfine coupling of the electron spin, S = 3/2, with the nuclear spin, I = 7/2, of ^{51}V.

Numerical simulations of an electron spin, S = 3/2, with electron-nuclear hyperfine interactions for a single vanadium ^{51}V ion (nuclear spin, I = 7/2, 99.75% isotopic abundance) provided an excellent fit of the experimental EPR spectrum of compound **1** in THF at 4 K (**Figure 3**). Experimental EPR parameters, such as, the electronic **g** tensor [g_X, g_Y, g_Z], hyperfine **A** tensor, [A_X, A_Y, A_Z], isotropic hyperfine coupling constant or Fermi contact interaction, A_{iso}, and the zero-field splitting parameters, D and E, that were extracted from simulations reflect the coordination environment of ^{51}V in compound **1**. The **g**-tensor of [2.047, 2.015, 1.95] that was obtained from the numerical simulation was consistent with a small rhombic symmetry for compound **1** and the numerically simulated spectrum using the magnetic parameters in **Table 1** is in excellent agreement with the experimental EPR spectrum (**Figure 3**).

The axial and rhombic zero-field splitting parameters, D and E, respectively, of the S = 3/2 ^{51}V ion of compound **1** were also obtained from the EPR spectral simulations. The ratio of the zero-field splittings, E/D, or rhombicity is important as it is a measure of the extent of deviation of the system from axial symmetry. In the presence of perfect axial symmetry, the ratio of the zero-field-splittings, E/D, is zero and in the presence of a completely rhombic symmetry, E/D = 1/3.[20] In the case of compound **1**, the zero-field-splitting parameters, D and E, were determined to be 2.66 cm^{-1} and 0.058 cm^{-1}, respectively, with an E/D ratio of 0.022. This was indicative of a nearly axial zero-field symmetry. In comparison with the rhombicity of the EPR spectrum that was previously observed for [V(DIPP)$_4$\{Li(THF)\}$_2$] (E/D ratio of 0.07),[13] compound **1** exhibits a smaller rhombic distortion which is supported by its E/D ratio of 0.022. The smaller ZFS rhombicity parameter for compound **1** can be

interpreted as an indication that both chiral (D_2-symmetric) V^{II} complexes are present in solution in near equal amounts considering that the original ligand, H$_2$TBDMPD, was racemic. On steric grounds, it is unlikely compound **1** displays fluxional behaviour in THF solution and improbable that the small rhombicity parameter can be attributed to **1** exhibiting square planarity, as that requires rotation of the biphenyl moiety through a high energy coplanar geometry. The ZFS parameters derived from the spectral simulations for compound **1** are in agreement with the hyperfine couplings previously reported for vanadium(II) species.[21-23]

DFT calculations were performed with the software program, ORCA 4.0[24,25] to calculate the magnetic parameters and better understand the electronic structure of compound **1**. It was previously demonstrated that the isotropic hyperfine coupling constant, A_{iso}, for V^{IV} species predicted by DFT depended on the exchange-correlation functional that was employed in the calculations.[26,27] This was because the isotropic or Fermi contact interaction, A_{iso}, is related to the electron spin density at the magnetic nucleus and inclusion of spin polarization effects of the core s-orbitals of vanadium were particularly important for the accurate prediction of A_{iso}.[28-31] Therefore, the functional and basis set that were used in this study were optimized by: (i) fixing the basis set and varying the functional (B3LYP, BHLYP, BHandHLYP, B3PW91 and ωB97X-D3), and (ii) fixing the functional and changing the basis set (6-311g(d,p), TZVP, QZVP, SVP and pc-3).

The suitable functional and basis set for the DFT calculations were determined by comparing the calculated and experimental hyperfine coupling constant, A_{iso}, for ^{51}V in compound **1** (Table S1).† A closer agreement between the predicted and experimental value of A_{iso} was obtained with a BHLYP correlation functional (a combination of Hartree-Fock theory and local DFT) with a pc-3 basis set.[32,33] This is in agreement with previous observations by Larsen and co-workers where Gaussian DFT calculations of A_{iso} with the hybrid functionals (BHLYP, BHP86, and BHPW91) yielded the best agreement with experimental results for $^{51}V^{IV}$ species.[28,29] The results are also consistent with Munzarova and Kaupp who observed that the calculated A_{iso} value for transition metal complexes depends on the functional and in the case of $^{51}V^{IV}$, the best quantitative agreement with the experimental A_{iso} was found with a hybrid functional as the mixing of exact exchange with the hybrid functional enhanced the spin polarization of s-type metal core orbitals.[27] In terms of the basis set, it was previously demonstrated that using a 6-311g(d,p) basis set in conjunction with the above functionals yielded deviations of ~5% and the use of more complete basis sets resulted in marginal improvement.[34]

The DFT calculations indicate that the unpaired electron spin density predominantly resides on the central V^{II} ion suggesting that the reactivity of the compound would likely be determined by the oxidation state of the metal ion rather than the coordination geometry (**Figure 4**). Moreover, the relative energies of the highest occupied MOs that are predominantly metal in character, e.g., d_{xy}, d_{xz}, and d_{yz}, differ only slightly in energy, with one MO lower in energy (-5.13 eV) relative to the other two occupied MOs that are

Table 1. Comparison of the dipolar and isotropic hyperfine coupling constants of compound **1** that were obtained from the *cw* EPR spectra (**Figure 3**) with the couplings predicted by DFT calculations using a BHLYP correlational functional with a pc-3 basis set.

Method	A$_x$ (MHz)	A$_y$ (MHz)	A$_z$ (MHz)	A$_{iso}$ (MHz)
EPR	-108.00	-55.00	-84.00	-82.30
DFT	-108.50	-28.33	-52.33	-63.05

COMMUNICATION   Chemical Communications

nearly degenerate and a bit higher in energy (-4.81 and -4.75 eV). The arrangement of these energy levels from the DFT calculations is consistent with orbital diagrams for distortion of a square planar to tetrahedral ML_4 complex as presented by Albright *et al*.[35]

While compound **1** is distinct from [V(DIPP)$_4${Li(THF)}$_2$] in terms of coordination geometry, spectroscopy, and steric considerations, e.g., four *tert*-butyl groups shield V^{II} as compared to eight isopropyl groups in [V(DIPP)$_4${Li(THF)}$_2$][13], the two compounds show similar reactivity based on preliminary studies with comparable substrates. Compound **1** reacts with CO at room temperature analogous to [V(DIPP)$_4${Li(THF)}$_2$], with ligand redistribution and redox chemistry such that the principal products obtained are [V(CO)$_6$]$^-$ (as confirmed by IR spectroscopy) and a V^{III} species as judged by an EPR-silent species at 77 K (most likely [V(TBDMPD)$_2$]$^-$).[13] Compound **1** is also highly sensitive to oxygen. A polyoxo V^V complex crystallized from a freshly prepared solution of [V(TBDMPD)$_2${Li(THF)}$_2$] that was inadvertently exposed to O$_2$ was identified by X-ray crystallography as [V$_3$Li$_2$(μ-TBDMPD)$_3$(μ-O)$_7$(μ-OTf){Li(THF)}$_2${Li(Et$_2$O)}$_2$]·Et$_2$O.§

Inspection of a space-filling model of the DFT structure of compound **1** indicates that V^{II} is shielded by a rather sterically demanding ligand environment, therefore reaction with 1,2-diphenylhydrazine is thought to proceed *via* outer sphere electron transfer. The addition of 1,2-diphenylhydrazine to a THF solution of Compound **1** resulted in isolation of [V(TBDMPD)$_2$], compound **2**, as thin brown rods after solvent removal, extraction with Et$_2$O, filtration, and standing at 0º C overnight. (*Note*: GC-MS of an acidified aqueous reaction mixture aliquot showed the reduction product to be aniline). The room temperature EPR spectrum of compound **2** using toluene as a solvent displayed an isotropic 8-line pattern at g = 1.974† which is typical of V^{IV}, as seen for V=O^{2+} species (Figure S1A).[36] Vanadium(IV) is characterized by a $3d^1$ electronic state and is an electron spin ½ system (S = ½). The 8-line spectrum is the result of the electron-nuclear hyperfine interaction of the electron spin, *S* = 1/2, with the nuclear spin, *I* = 7/2, of ^{51}V. A frozen solution of compound **2** in toluene at 9 K displayed a rigid-lattice spectrum (Figure S1B) that allowed for the determination of the **g**- and **A** tensor through numerical simulations.†
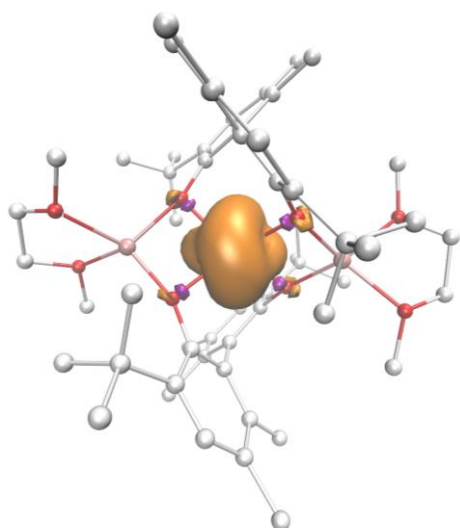

Figure 4. The overall unpaired electron spin density distribution in compound **1** as observed in the DFT calculations (BHLYP with pc-3 basis). Electron spin density is primarily localized on the V^{II} ion with a very small amount of the spin density delocalized on the oxygen atoms coordinated to the V^{II} ion. Hydrogen atoms omitted for clarity.
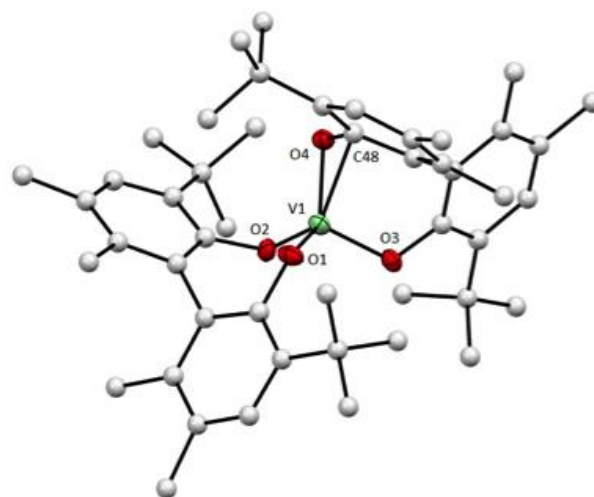

Figure 5. The X-ray crystal structure of compound **2** with thermal ellipsoids at 50% probability of all non-carbon atoms for clarity (hydrogen atoms omitted). Selected interatomic bond lengths [Å] and angles [deg]: V1-O4 1.822(4), V1-O3 1.812(4), V1-O1 1.804(4), V1-O2 1.805(4), V1··C48 2.343(6), O1-V1-O2 107.1(2), O3-V1-O4 111.3(2), O1-V1-O3 112.9(2), O2-V1-O4 105.9(2), O1-V1-O4 116.8(2), O2-V1-O3 101.2(2), C48-O4-V1 93.0(3).

The crystal structure of compound **2** is presented in **Figure 5** with a list of selected bond distances and bond angles.†

The most remarkable feature of compound **2** is the phenolate ring of O4 which is 'folded-over' the V^{IV} center. The V1-O4-C48 angle is rather acute (93º) compared to the average of the remaining V-O-C$_{aryl}$ angles (118º). The distance between V1··C48 (2.343(6) Å) indicates an η^2 bonding mode for this phenolate group bound to vanadium (**Figure 5**). The interaction produces a metallacyclopropane comprising the V-O-C$_{aryl}$ moiety with an acute C48-V1-O4 angle of 36º. According to the CSD[16] this type of η^2 bonding mode is very rare.[37,38]

In conclusion, the combination of experimental and DFT methods presented in this work demonstrate that a greater level of clarity for the high reactivity of unusually distorted V^{II} species can be achieved when both EPR spectroscopy and DFT are used in conjunction with each other. In the future, we plan to probe additional reactivity of compound **1** by lithium ion removal/sequestration and also the coordination chemistry of reactivity of V^{II} with less sterically encumbered biphenolate ligands.

Conflicts of interest

There are no conflicts to declare.

Acknowledgements

Notes and references

‡ [V(THF)$_4$(CF$_3$SO$_3$)$_2$] was prepared by reduction of V(CF$_3$SO$_3$)$_3$ using metallic zinc and was isolated in 85% yield as light blue crystals. This compound has been characterized by X-ray crystallography.[13]

§ Characterization of this degradation product is limited, however X-ray crystallography established structural identity as a trinuclear species found to crystallize in the triclinic space group P-1, with a = 15.550(5) Å, b = 15.686(8) Å, c = 23.728(8) Å, α = 79.70(2)º, β = 85.31(2)º, γ = 75.70(2)º, V = 5514(4) Å^3, and Z = 2. Diffraction data were collected at 183 K by using Mo K_α radiation out to 2θ = 45º yielding 10,162 independent reflections.

1   A. F. Shestakov and A. E. Shilov, *Kinetics and Catalysis* (Translation of Kinetika i Kataliz), 2001, **42**(5), 653.

2   T. A. Bazhenova and A. E. Shilov, *Coord. Chem. Rev.,* 1995, **144**, 69.

3   J. Y. Becker and B. J. Posin, *Electroanal. Chem. Interfacial Electrochem.,* 1988, **250**, 385.

4   N. P. Luneva, A. P. Moravskii, and A. E. Shilov, *Nouv. J. Chim.,* 1982, **6**, 245.

5   N. P. Luneva, L. A. Nikonova, and A. E. Shilov, *Kinet. Katal.,* 1980, **21**, 1458.

6   N. P. Luneva, L. A. Nikonova, and A. E. Shilov, *React. Kinet. Catal. Lett.,* 1976, **5**, 149.

7   L. A. Nikonova, N. I. Pershikova, S. A. Isaeva, A. G. Ovcharenko, and A. E. Shilov, *Tezisy Dokl. - Vses. Chugaevskoe Soveshch. Khim. Kompleksn. Soedin. 12th,* 1975, **2**, 184.

8   L. A. Nikonova, A. G. Ovcharenko, O. N. Efimov, V. A. Avilov, and A. E. Shilov, *Kinet. Katal.,* 1972, **13**, 1602.

9   Y. Sekiguchi, K. Arashiba, H. Tanaka, A. Eizawa, K. Nakajima, K. Yoshizawa, and Y. Nishibayashi, *Angew. Chem.*, 2018, **130**, 9202.

10 W.-C. Chu, C.-C. Wu, and H.-F. Hsu, *Inorg. Chem.,* 2006, **45**, 3164.

11 J. N. Boynton, J.-D. Guo, J. C. Fettinger, C. E. Melton, S. Nagase, and P. P. Power, *J. Am. Chem. Soc.* 2013, **135**, 10720.

12 B. L. Tran, B. Pinter, A. J. Nichols, F. T. Konopka, R. Thompson, C.-H. Chen, J. Krzystek, A. Ozarowski, J. Telser, M.-H. Baik, K. Meyer, and D. J. Mindiola, *J. Am. Chem. Soc.,* 2012, **134**, 13035.

13 M. J. Scott, W. C. A. Wilisch and W.H. Armstrong, *J. Am. Chem. Soc.*, 1990, **112**, 2430.

14 L. Wang, X. Pan, L. Yao, N. Tang, and J. Wu, *Eur. J. Inorg. Chem.*, 2011, **5**, 632-636. The ligand is 3,3',5,5'-tetra-*tert*-butyl substituted biphenolate known as H$_2$TBBP and the Zn^{II} complex is [Zn(TBBP)$_2${Li(THF)$_2$}$_2$].

15 S. Keinan and D. Avnir, *Inorg. Chem.*, 2001, **40**, 318.

16 The collection of structural data was obtained through systematic searches of the Cambridge Structural Database, F. H. Allen, and O. Kennard, *Chem. Des. Automat. News*, 1993, **8**, 31.

17 A. F. Cozzolino, J. S. Silvia, N. Lopez and C. C. Cummins, *Dalton Trans.*, 2014, **43**, 4639.

18 R. K. Minhas, J. J. H. Edema, S. Gambarotta and A. Meetsma, *J. Am. Chem. Soc.*, 1993, **115**, 6710.

19 S. Alvarez, P. Alemany, D. Casanova, J. Cirera, M. Llunell, and D. Avnir, *Coord. Chem. Rev.*, 2005, **249**, 1693.

20 A. Abragam and B. Bleaney, Eds., Electron paramagnetic resonance of transition ions, 1970, Dover, New York.

21 R. Prins, P. Biloen and J. D. W. van Voorst, *J. Chem. Phys.*, 1967, **46**, 1216.

22 R. Prins and J. D. W. van Voorst, *J. Chem. Phys.*, 1968, **49**, 4665.

23 J. Krzysteka, A. Ozarowski, J. Telser and D. C. Crans, *Coord. Chem. Rev.,* 2015, **301-302**, 123.

24 F. Neese, *Wiley Interdiscip. Rev.-Comput. Mol. Sci.*, 2012, **2**, 73.

25 F. Neese, Wiley *Interdiscip. Rev.-Comput. Mol. Sci.*, 2018, **8**, e1327.

26 P. Nachtigall *et al.*, *Chem. Phys.*, 2004, **305**, 291.

27 M. L. Munzarova´and M. Kaupp, *J. Phys. Chem. A*, 1999, **103**, 9966.

28 A. C. Saladino and S. C. Larsen, *Catal. Today*, 2005, **105**, 122.

29 A. C. Saladino and S. C. Larsen, *J. Phys. Chem. A*, 2003, **107**, 1872.

30 M. Stein, E. van Lenthe, E.J. Baerends and W. Lubitz, *J. Phys. Chem. A*, 2001, **105**, 416.

31 M. L. Munzarova´, and M. Kaupp, *J. Phys. Chem. B*, 2001, **105**, 12644.

32 A. D. Becke, *J. Chem. Phys.*, 1993, **98**, 1372.

33 F. Jensen, *J. Chem. Phys.*, 2001, **115**, 9113.

34 G. Micera and E. Garribba, *Dalton Trans.*, 2009, **11**, 1914.

35 T. A. Albright, J. K. Burdett, and M.-H. Whangbo, Orbital Interactions in Chemistry·, John Wiley and Sons: New York, 1985; p 305.

36 J. E. Wertz and J. R. Bolton, Electron spin resonance, 1986, Chapman and Hall, New York.

37 H. Kawaguchi and T. Matsuo, *J. Am. Chem. Soc.*, 2003, **125**, 14254.

38 R. Qi, B. Liu, X. Xu, Z. Yang, Y. Yao, Y. Zhang, and Q. Shen, *Dalton Trans*., 2008, 5016.